Deliquescence, Efflorescence, and Water Activity in Ammonium Nitrate and Mixed Ammonium Nitrate/Succinic Acid Microparticles

James M. Lightstone, Timothy B. Onasch, and Dan Imre*

Atmospheric Sciences Division, Environmental Sciences Department, Brookhaven National Laboratory, Upton, New York 11973

Susan Oatis

Natural Science Division, Southampton College, Long Island University, Southampton, New York 11968

Received: June 13, 2000; In Final Form: August 23, 2000

We have investigated the thermodynamics and kinetics of ammonium nitrate/water and mixed ammonium nitrate/succinic acid/water microparticles. The water activity of ammonium nitrate microparticles is determined as a function of composition down to 12% relative humidity by accounting for the rapid evaporation of ammonia and nitric acid. Both the observed deliquescence and water activities for ammonium nitrate/water microparticles are found to be in good agreement with predicted values. Supermicron ammonium nitrate particles generated from high-purity methanol are found not to effloresce, but form an anhydrous liquid state observed only in particle form. We also present data on the hydroscopicity and phase transitions of internally mixed ammonium nitrate/succinic acid particles. A pronounced reduction in the particle growth factor at deliquescence is reported, indicating that the succinic acid does not take up a significant amount of water. Additionally, the deliquescence relative humidity is found to decrease slightly as the mass percent of succinic acid is increased from 12.5 to 50%. Solid succinic acid in ammonium nitrate drops acts to catalyze efflorescence of ammonium nitrate at high relative humidity. However, when the relative humidity is increased sufficiently to completely dissolve the succinic acid, no efflorescence is observed. The resulting data are analyzed using classical nucleation theory to derive the free energy barrier to nucleation, the critical supersaturation, the size of the critical nucleus, and the contact parameter between ammonium nitrate crystal and the solid succinic acid.

1. Introduction

Atmospheric aerosols have a direct impact on the earth's radiation balance, an effect opposite in sign to that of the greenhouse gases. By scattering incoming solar radiation, either directly or indirectly as cloud particles, aerosols exert a cooling effect on the earth's climate. In addition, they may provide catalytic sites for heterogeneous reactions to occur. The extent to which atmospheric particles will scatter light and be chemically reactive is directly related to their size, composition, and physical state. Tropospheric aerosols, both natural and anthropogenic in origin, are mostly composed of hygroscopic inorganic salts such as ammonium nitrate yet may contain organic compounds. These mixed particles may behave quite differently from the pure particles under changing relative humidity (RH) conditions. Therefore, in order to gain an understanding of these atmospheric processes and provide accurate input for regional climate models, it is imperative to understand the thermodynamics and kinetics of internally mixed particles under variable atmospheric conditions.

It has been well established that the majority of ambient aerosol mass is composed of inorganic sulfates, nitrates, and chlorides. One of the most common constituents of atmospheric aerosols is ammonium nitrate, the vast majority of which is of anthropogenic origin.[1,2] Ammonium nitrate forms in the atmosphere by two mechanisms. In the gas phase it is produced when OH oxidizes NO_x to nitric acid, which in the presence of ammonia is neutralized to ammonium nitrate. In the absence of sunlight, NO_2 can react with NO_3 to form N_2O_5, which is heterogeneously converted to nitric acid in the presence of hydrated aerosols. Unlike most of the other hygroscopic salts that are found in the atmosphere, ammonium nitrate is a salt with a relatively high vapor pressure. Particles containing ammonium nitrate are in equilibrium with $NH_{3(g)} + HNO_{3(g)}$ and the partitioning between particle and gas is a strong function of temperature and relative humidity. Because of its volatility, ammonium nitrate is very difficult to study and thus has been the subject of a few rather limited studies of its hydration and dehydration properties.

Recently we have come to realize that aside from the inorganic fraction, many atmospheric aerosols contain a significant fraction of organic compounds. However, mostly due to the lack of thermodynamic data, many current aerosol models[3] include only inorganic salts. This may represent a significant omission since atmospheric aerosols are found in many areas to contain 20−50% organic compounds by mass.[4−6] The organic fraction is expected to have a profound impact on the light scattering, hydroscopicity, and phase transition properties of these multicomponent aerosols.

Organic compounds covering a wide range of carbon numbers and functional groups have been identified in smog chamber experiments[7,8] and field studies,[4,9−12] of which dicarboxylic acids[13−19] are some of the most commonly found. Originating

* Corresponding author.

10.1021/jp002137h CCC: $19.00
Published on Web 09/27/2000

from natural and anthropogenic sources, these acids can range in size from C_2-C_{10} and in solubility.[20] They exist in the atmosphere as a result of direct emission or by oxidation of more volatile compounds. Because of their low vapor pressure they tend to condense on preexisting atmospheric particles. It is not uncommon to find atmospheric particles composed of a mixture of inorganic acids or salts with organic compounds. As the inorganic fraction deliquesces to form a droplet the less soluble organic acids remain as solid inclusions within the droplet or coat the particle by forming a film over the surface.

When mixed with common hygroscopic inorganic species, organic compounds induce substantial changes in the thermodynamic as well as the kinetic properties of atmospheric aerosols. Studies have shown that hydration behavior and light scattering properties of aerosol droplets[21−30] are sensitive to the presence of organics. Most of the studies to date focus on the presence of the organic as a film over the aerosol surface with little or no emphasis on internally mixed insoluble organic/inorganic aerosols.

One of the unique properties of single-component microdroplets is their tendency to form metastable supersaturated solutions as the relative humidity is decreased. This is a consequence of a kinetic barrier to nucleation. Studies[31,32] have shown that the presence of inorganic solid inclusions in microdroplets catalyzes efflorescence (via heterogeneous nucleation) and thus significantly increases the RH at which liquid−solid transitions occur. Therefore, the presence of a solid organic compound within a solution droplet may also provide a surface that can heterogeneously catalyze the crystallization of the soluble fraction.

In this paper we present a study of single suspended microparticles composed of ammonium nitrate, and ammonium nitrate mixed with succinic acid (AN/SA). We have investigated the deliquescence, efflorescence, and water activity of ammonium nitrate at 298 K. We have also investigated the effects of succinic acid on the thermodynamics and kinetics of ammonium nitrate. Succinic acid is a slightly soluble, 8.6 g/100 g H_2O at 298 K,[20] C_4 dicarboxylic acid that has been detected in several of the field studies mentioned above. Because of its low solubility, most succinic acid will remain a solid after ammonium nitrate has become a solution droplet. Therefore, we have quantified the effects of solid succinic acid on the phase transitions and hygroscopicity of ammonium nitrate. In addition, at high RH it is possible to completely dissolve the succinic acid to produce a homogeneous droplet containing ammonium nitrate/succinic acid/water. Since no solid inclusion is present under these conditions, liquid solution droplets supersaturated with respect to both ammonium nitrate and succinic acid can be formed.

2. Experimental Section

An electrodynamic balance, described in detail elsewhere,[33,34] mounted in a temperature-controlled vacuum chamber was used to obtain all data at 298.2 ± 0.2 K. While open to ambient air, the entire chamber is continuously flushed with dry nitrogen gas in order to minimize gaseous and particulate contaminates. In each experiment a charged solution droplet is introduced into the cell by a simple electrospray technique. The droplet is trapped at the center of the ac ring electrode, and balanced against gravity by the dc voltage applied across the two cap electrodes. The particle is illuminated by a He−Ne laser and viewed using a charged coupled device (CCD) and a TV. The light scattered by the particle is collected at 90° from the laser beam by a photomultiplier to record changes in light scattering intensity as a function of RH and therefore particle phase and size. We denote the presentation of such data as a Mie spectrum. Once a particle has been centered in the null point of the cell the chamber is evacuated to 10^{-6} Torr. The RH of the system is controlled by addition or removal of water vapor through a variable leak valve. The water pressure is directly measured with a Baratron capacitance manometer. Single-particle Raman spectra were obtained using an argon ion laser at 514.5 nm and a 1 m double monochromator equipped with a liquid nitrogen cooled CCD detector. A detailed description of the single-particle Raman system was presented earlier.[35] All solutions were prepared with high-purity ammonium nitrate (Puratronic-Alfa Aesar) in purge and trap grade methanol (Fisher Scientific) and filtered through 20 nm pore size filters upon transfer to the particle delivery device. Solutions, 4 wt % of solute, were used, with varying AN/SA (Aldrich) ratios in the organic studies.

3. Results and Discussion

3.1 Deliquescence and Water Activity. 3.1.1. Ammonium Nitrate/Water. Before the effects of succinic acid on the kinetics and thermodynamics of ammonium nitrate particles can be quantified, hydroscopicity and phase transitions must first be defined for the binary ammonium nitrate/water system. Ammonium nitrate is a major component of atmospheric aerosols.[1,2,36,37] Despite its relevance to the atmosphere, few laboratory studies of ammonium nitrate particles have been presented.[38−41] Due to its volatility and sensitivity to impurities, ammonium nitrate has been an enigma to the atmospheric aerosol community, especially with respect to ambient aerosol sampling techniques. Similarly, very little laboratory data are available for ammonium nitrate droplets at RH below the deliquescence point.

The deliquescence relative humidity (DRH) of ammonium nitrate at 298 K can be predicted on the basis of thermodynamics. Tang[39] calculated a DRH of 62% while a more recent multicomponent, mole-fraction-based thermodynamic model[3] predicts a DRH of 61.5% in agreement with observations in the bulk by Edgar and Swan[42] and in particle form by Tang[38] and Richardson and Hightower.[43] In contrast, only three studies to our knowledge report information on the activities and vapor pressures (VP) of ammonium nitrate supersaturated solution droplets. Tang[39] reported one of the first hydration curves for an ammonium nitrate particle. While the experimental data appears to follow the predicted water activity measured over bulk solutions at and above the saturated concentration (deliquescence point) it does not provide a clear picture in the supersaturated region. Richardson and Hightower[43] reported observations and evaporation rates for crystalline ammonium nitrate particles and metastable liquid ammonium nitrate droplets at ∼0% RH, a state they termed anhydrous liquid. In 1992, Chan et al.[40] mapped out the water uptake curve for ammonium nitrate particles to ∼30% RH, where efflorescence was observed. These studies may have been hampered by the presence of impurities that limited the degree of supersaturation that could be achieved. Here we report data on the full water uptake curve for supersaturated ammonium nitrate droplets.

Results from the present study of a complete hydration/dehydration cycle at 298 K of an ammonium nitrate solution droplet are shown in Figure 1A. The hydration path exhibits common behavior with a very sharp deliquescence transition at 61.8 ± 0.3% in agreement with both calculated and experimentally determined values. The dehydration part of the cycle is much more complex. This portion of the run, presented in Figure 1A as open squares, begins at 64% RH and terminates

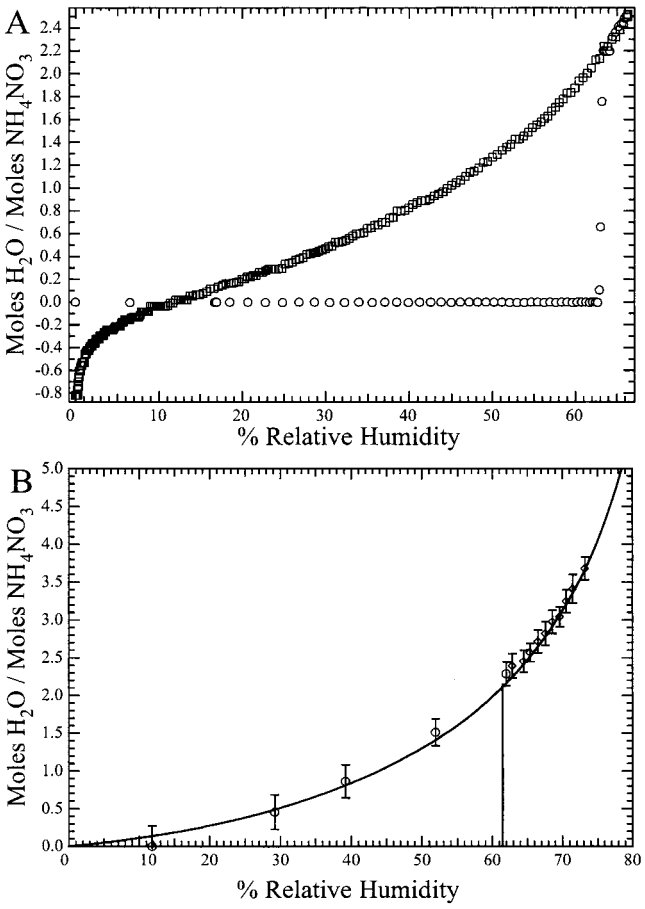

Figure 1. (A) hydration (open circles)/dehydration (open squares) cycle for an ammonium nitrate particle that does not effloresce. Note that the dehydration cycles ends with an apparent negative mass due to the evaporation of NH_3 and HNO_3 evaporation. (B) Water activity curve for ammonium nitrate obtained by correcting for evaporation (open circles and diamonds). Clegg et al.[3] thermodynamic model predictions for ammonium nitrate at 298 K are shown for comparison (solid line).

at a measured absolute pressure of 1×10^{-5} Torr with the particle in an anhydrous liquidlike state at ~0% RH. As mentioned above, Richardson and Hightower[43] have previously observed this behavior. No efflorescence was observed nor could be induced with time or by repeated humidification/dehydration cycling.

A second obvious feature of the hydration/dehydration cycle shown in Figure 1A is that the composition of the particle, as determined by particle mass changes, ends below the starting point. This loss of mass is indicative of a significant evaporation of ammonium nitrate by the end of the run. As the figure clearly demonstrates, ammonium nitrate has sufficiently high VP of HNO_3 and NH_3 as to make particle evaporation significant on the time scales of typical single-particle experiments. Therefore, the commonly invoked assumption in this type of experiment, that the total solute mass remains constant throughout an experiment, may not be valid. The evaporation of solid and liquid ammonium nitrate particles below and above the DRH, respectively, have been investigated.[44,45] The VP of HNO_3 and NH_3 over ammonium nitrate solutions was found to be a strong function of the droplet composition and therefore the RH, decreasing rapidly with increasing RH.[46,47] However, no systematic data of HNO_3 and NH_3 vapor pressure over supersaturated ammonium nitrate solution droplets as a function of RH (solution composition) are presently available. A measure of the dependence of ammonium nitrate VP on the RH over metastable solutions can be inferred from the observations by Richardson and Hightower[43] for ammonium nitrate solution droplets at 0% RH and those by Chan et al.[40] at 30% RH. The former found an evaporation rate almost 20 times faster than the solid, while the latter observed no significant loss of mass during 4−6 h runs.

We conclude that the high volatility of HNO_3 and NH_3 at low RH necessitates the development of a technique allowing us to correct for the loss of ammonium nitrate mass in order to be able to derive water activity curves. Based on evaporation experiments carried out in our laboratory, to be presented separately, we determine that on the time scale of our experiments evaporation of solid ammonium nitrate at all RH and evaporation of ammonium nitrate solution droplets above 40% RH is insignificant. Therefore, we set a point above 40% RH as a reference. The RH is then dropped below 40%, a data point is taken, and the RH is returned to the set reference point in a timely manner. Assuming the time taken to decrease and increase the RH are equal, we can take half of the difference in mass between the initial and final reference points and apply this as a correction to the acquired data point. By repeating this procedure at several RHs we were able to map out the corrected water activity curve below the deliquescence point. The results obtained using this technique are presented in Figure 1B and in Table 1. The experimental data indicate a rapidly decreasing water content as the RH decreases over supersaturated ammonium nitrate droplets, ending with very little water present in the liquid below 12% RH. A theoretical curve based on the model of Clegg et al.[3] is shown for comparison. The model fits our data well over the full relative humidity range and therefore will be used in the following sections to calculate the uptake curve for ammonium nitrate droplets.

3.1.2. Ammonium Nitrate/Succinic Acid/Water. Internally mixed AN/SA particles were produced from solutions containing 4% solute by mass, where the solute consisted of varying amounts of ammonium nitrate and succinic acid. Single-particle Raman spectroscopy was used to confirm that we had indeed produced internally mixed particles. Figure 2 shows Raman spectra for (A) bulk ammonium nitrate crystals, (B) a mixed dry solid AN/SA particle, and (C) bulk succinic acid crystals. Spectrum (B) obviously contains the same features as (A) + (C). The fact that the ammonium nitrate peak in (B) has not dramatically broadened in comparison with the corresponding bulk peak in (A), indicates the ammonium nitrate and succinic acid have not reacted to form large amounts of ammoniated succinate salts. Rather, the mixed particle has solidified into separate crystallites of ammonium nitrate and succinic acid. In support of these observations, using K_a's from Harris [48] we estimate that approximately 2% of the initial succinic acid may react and form ammoniated succinate salts. While such an amount is below our Raman spectroscopy detection limit, these additional salts may complicate the thermodynamics of the ammonium nitrate/succinic acid/water system.

The hydration and dehydration curves of binary ammonium nitrate/water[3] and tertiary ammonium nitrate/succinic acid/water particles, composed of 12.5%, 25%, and 50% SA by mass, are shown in Figure 3A. Also shown is the water activity curve of succinic acid derived from Na et al.[49] As expected, the presence of the relatively insoluble organic acid decreases the growth factor as measured by the mass ratio of the solution droplet to the dry particle, M/M_0. The measured M/M_0 for all particle compositions at their respective deliquescence points are given in Table 1 for reference. A similar trend of decreased water uptake observed in ambient aerosols has been interpreted as signifying the presence of organic compounds.[22,50,51]

TABLE 1: Experimental Data Points from Figure 1B and Figure 4

ammonium nitrate		12.5% SA		25% SA		50% SA	
water activity	mole ratio[a]	water activity	mole ratio[a]	water activity	mole ratio[a]	water activity	mole ratio[a]
0.732	3.7 ± 0.2	0.45	1.0 ± 0.1	0.50	1.6 ± 0.1	0.45	1.4
0.715	3.4 ± 0.2	0.50	1.3 ± 0.1	0.55	1.9 ± 0.2	0.50	1.5
0.706	3.2 ± 0.2	0.55	1.6 ± 0.1	0.60	2.5 ± 0.2	0.55	1.9 ± 0.2
0.697	3.0 ± 0.1	0.60	2.0 ± 0.2	0.65	3.0 ± 0.2	0.60	2.3 ± 0.1
0.686	2.9 ± 0.2	0.65	2.6 ± 0.2	0.70	3.9 ± 0.2	0.65	2.9 ± 0.2
0.676	2.8 ± 0.2	0.70	3.4 ± 0.2	0.75	5.1 ± 0.2	0.70	3.7 ± 0.2
0.665	2.7 ± 0.2	0.75	4.4 ± 0.2	0.80	7.1 ± 0.3	0.75	4.9 ± 0.3
0.654	2.6 ± 0.1	0.80	6.3 ± 0.4	0.85	10.1 ± 0.4	0.80	6.8
0.645	2.5 ± 0.2			0.90	16.2 ± 0.2	0.85	9.5
0.629	2.4 ± 0.2					0.90	15.5
0.620[b]	2.3 ± 0.2					0.95	38.8
0.519[b]	1.5 ± 0.2						
0.392[b]	0.8 ± 0.2						
0.292[b]	0.5 ± 0.2						
0.118[b]	0.0 ± 0.3						

[a] Moles of water/moles of ammonium nitrate. [b] Data obtained using the procedure to account for the evaporation of ammonium nitrate described at the end of section 3.1.1.

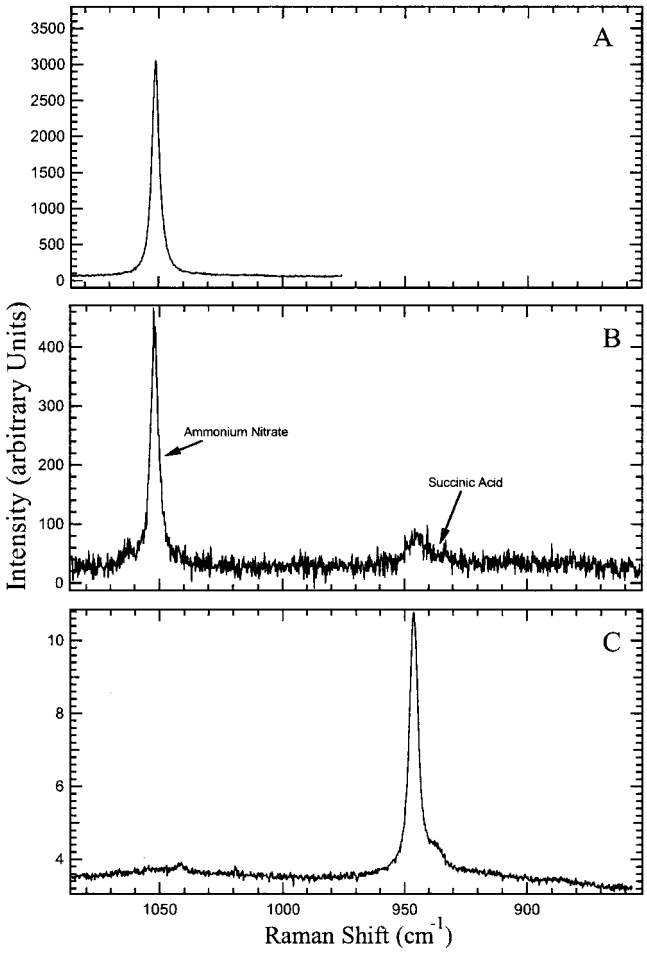

Figure 2. Raman spectra of (A) bulk ammonium nitrate, (B) mixed ammonium nitrate/succinic acid particle, and (C) bulk succinic acid.

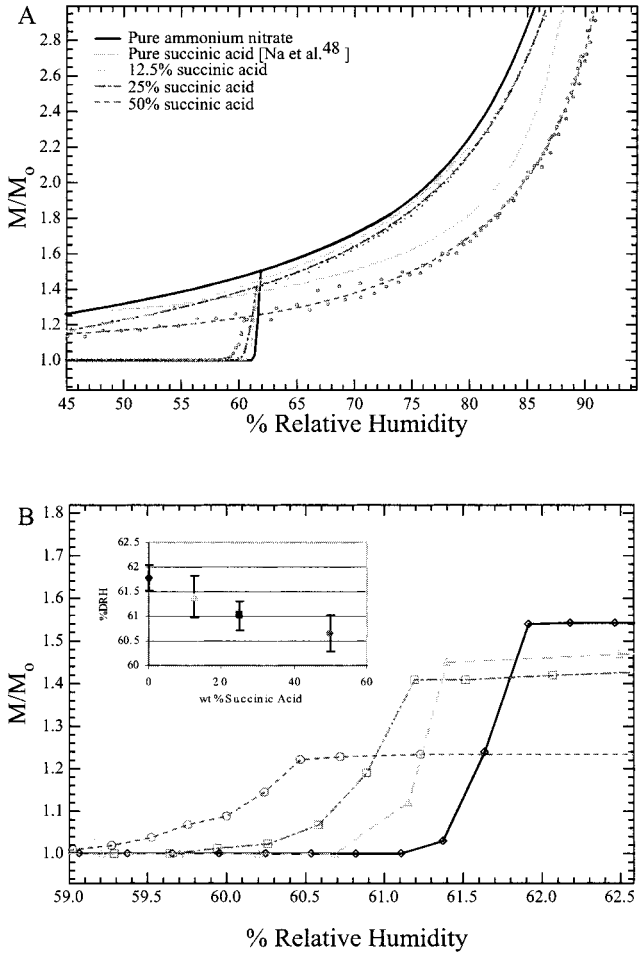

Figure 3. (A) hydration/dehydration curves for ammonium nitrate (from a best fit line through experimental data in Figure 1B, and continued from 73% RH using model from Clegg et al.[3]) and mixed AN/SA particles composed of 12.5%, 25%, and 50% succinic acid. Also shown is the water activity curve for supersaturated succinic acid from Na et al.[49] (B) an expanded view of (A) showing the deliquescence transitions in detail. The inset in (B) shows DRH versus SA composition.

The expanded view of the deliquescence region, Figure 3B, shows that there is a slight decrease (~1% RH) in the observed DRH of the mixed AN/SA particles (Note that the displayed curves are from individual particle runs.) Tang and Munkelwitz[33,52] and Wexler and Seinfeld[53] showed that a ternary salt and water mixture deliquesces at the eutonic point regardless of the initial dry salt composition. Therefore, we would expect our mixed AN/SA particles to deliquesce at the equilibrium RH of the eutonic solution, which is lower than the DRH for the binary ammonium nitrate/water system, regardless of the AN/SA composition. However, Tang and Munkelwitz[54] have also shown that the amount of water taken up at the deliquescence point of mixed ternary system is dependent upon the initial dry

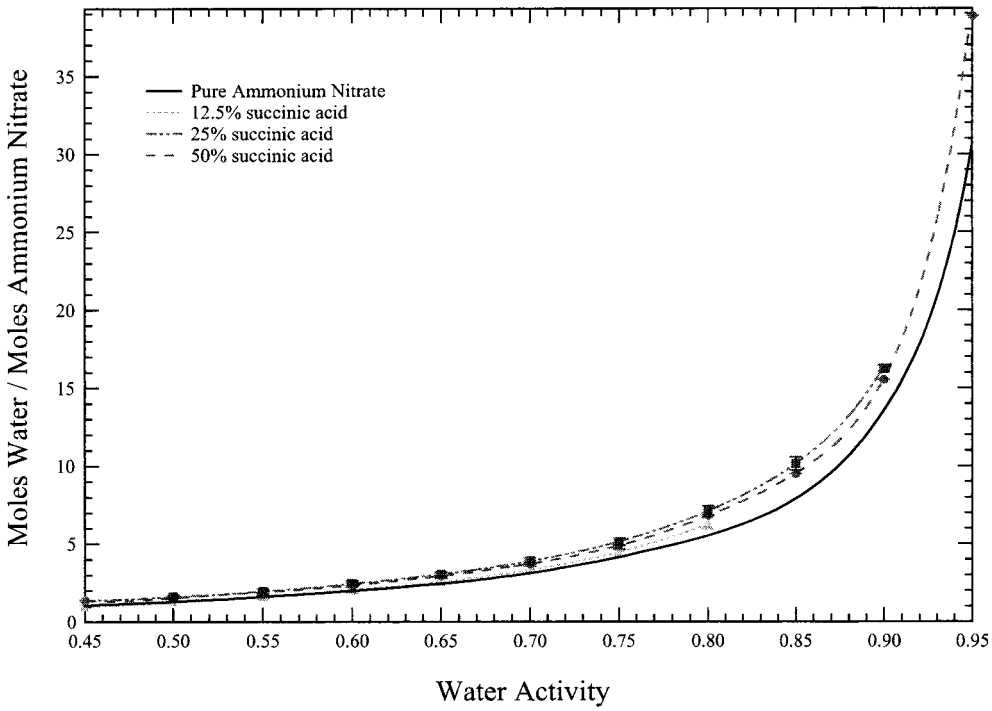

Figure 4. Water activity curves for ammonium nitrate[3] and mixed AN/SA particles composed of 12.5%, 25%, and 50% succinic acid by mass. The dashed lines are added to aid in distinguishing between the different compositions and are not fits.

salt composition. In the present case, the succinic acid is only slightly soluble and thus we believe the amount of water taken up at the eutonic point to be very small. On the basis of the lack of a defined eutonic transition prior to the deliquescence transition during the hydration runs in Figure 3, we conclude that the amount of water take up at the eutonic point is below our detection limit and the sharp transitions shown in Figure 3 are due to the deliquescence of the remaining solid ammonium nitrate.

The inset in Figure 3B illustrates the relationship between the observed DRH and the weight percent of succinic acid for all particles. In order for the DRH to be lowered, the VP of the saturated solution must also be lowered.[55] An increase in the number of succinic acid species in solution will lower the VP of the mixed AN/SA solution; however, the presence of solid succinic acid suggests that a solution saturated with respect to succinic acid exists in all cases. Therefore, we would not expect the DRH to drop as a function of the initial particle composition, as we have observed. A complication in the present case is the possible formation of a four- or five-species solution due to the formation of ammoniated succinate species. With little thermodynamic data available for these salts it is difficult to determine the amount of salts formed and whether this may account for the observed trend in DRH. It is interesting to note that Andrews et al.[29] have observed a similar trend of decreasing DRH for mixed sodium chloride/Tween 80 particles.

Our particle generation and observation techniques allow the composition of the particle, described as the mole ratio of water to ammonium nitrate and/or succinic acid, to be accurately determined. The two assumptions made in this calculation are that the particles produced have the same AN/SA composition as the initial solutions and that the solutes (ammonium nitrate and succinic acid) do not significantly evaporate during the time scales of an experiment. Based on the preceding section and the known VP of solid succinic acid,[56] we believe that both assumptions are valid at RH $\geq$ 30% and when the particles are crystalline. Therefore, the M/M_0 ratio for the different water uptake curves shown in Figure 3 can be converted into the mole ratio of water to ammonium nitrate. Derived mole ratios of water to ammonium nitrate for the three AN/SA compositions are shown in Table 1 with each point representing average mole ratios from 4 to 6 different particles. Figure 4 illustrates these points along with the mole ratio for the binary ammonium nitrate/water system[3] for comparison. In this coordinate system all three curves for mixed solution droplets lie slightly above that of the ammonium nitrate, especially at higher relative humidities, suggesting that only a very small amount of the succinic acid is in solution at and below the deliquescence point. Since a solid organic core is present in all of the mixed particles and the crystalline succinic acid must be in equilibrium with the solution, the three curves should be identical. Therefore, the spread in the three curves gives an estimate of our experimental reproducibility.

Various methods have been used to model the thermodynamic properties of mixed component solutions.[3,57,58] These methods concentrate on modeling the thermodynamics of electrolytes in mixed solutions at high concentrations. In the present case, however, succinic acid solubility is pH dependent and may not dissociate in solution. It is important that such behavior be taken into account when forming new models. Important information for such a method is the water activity of the mixed solution as a function of composition, which can be used to determine the activities of the solutes through the Gibbs−Duhem relation. Therefore, we provide the following fit to all data points, which represents the particle composition, moles of ammonium nitrate/kg of H_2O, of a mixed AN/SA solution as a function of the water activity

$$m = \sum B_i a_w^i \qquad (1)$$

where m is the molality of ammonium nitrate in a mixed succinic acid/ammonium nitrate solution saturated with respect to succinic acid, a_w is the water activity, and B_i is the coefficient of the ith term in the polynomial expression. The derived coefficients are $B_0 = 823.49$; $B_1 = -4979.2$; $B_2 = 12\,997$; $B_3 = -17\,473$; $B_4 = 11\,818$; and $B_5 = -3188.2$.

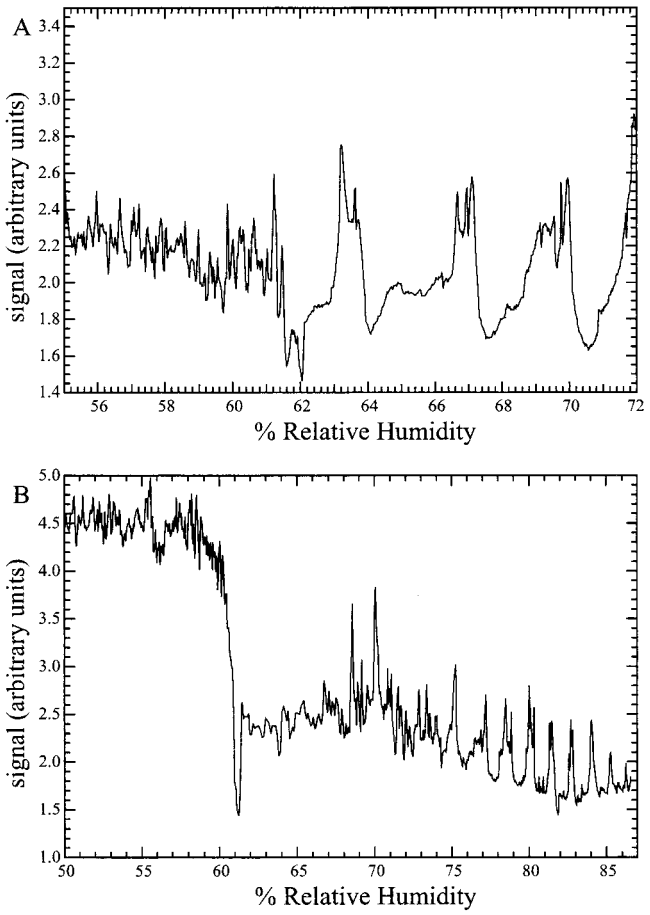

Figure 5. Mie-scattering versus increasing RH for (A) ammonium nitrate, and (B) mixed AN/SA particles with 25% SA by mass. Note that the x-axes of (A) and (B) have different scales.

The presence of the solid succinic acid impacts the light-scattering properties as well. Figure 5A shows a Mie spectrum obtained during a hydration experiment for an ammonium nitrate particle as a function of RH. Below 61.6% RH the particle is solid and the pattern is one of random high-frequency signal. Immediately following the deliquescence a homogeneous liquid drop forms and a drastic change in the Mie scattering spectrum is observed. The high-frequency random signal gives way to a well-defined smooth spectrum of scattered light intensity as a function of RH. In contrast with the ammonium nitrate droplet, Figure 5B shows a Mie spectrum for a mixed AN/SA particle, 25% SA by mass. The deliquescence at ~61% is clearly marked by a sudden drop in signal intensity, but because the droplet formed contains a seed sufficiently large to interact with the He−Ne laser light, the observed Mie signal is a combination of a Mie spectrum from a spherical particle and the random high-frequency signal characteristic of a solid, nonspherical particle. As the RH is increased, more succinic acid is dissolved and the solid inclusion becomes smaller until ~74% RH it becomes too small to affect the scattering of the 632 nm wavelength light.

3.2. Efflorescence. 3.2.1. Ammonium Nitrate/Water. Few studies have reported efflorescence relative humidity (ERH) values for ammonium nitrate/water particles. The literature values available appear to be contradictory. Chan et al.[40] observed efflorescence at ~30% RH, in agreement with the reported efflorescence range of 25-32% RH by Tang.[38] In contrast, ammonium nitrate particles exhibiting no crystallization have been reported by Cziczo and Abbatt,[41] Dougle et al.,[59] Tang,[39] and Richardson and Hightower.[43]

In an attempt to resolve this issue, we have conducted experiments on a large number of particles prepared through a variety of methods. We find that when ammonium nitrate microparticles were generated from a water-based solution a wide interparticle range of efflorescence points (0−30% RH) was observed. We have tested several sources of water (deionized and filtered Millipore water; HPLC grade water) and a variety of solution preparation procedures (no filtering; solutions filtered at 100, 50, and 20 nm; solutions filtered twice). The variation in ERH from one particle to the next was large and invariant of water source or treatment. Although efflorescence is a kinetically controlled process, the magnitude of the observed range of ERH is inconsistent with our understanding of the kinetics of homogeneous nucleation.

To determine whether the observed effect is due to impurities and therefore heterogeneously driven, we have investigated the variability in ERH for *individual* particles cycled repeatedly through deliquescence and efflorescence. The data show that when an *individual* particle was taken through the cycle several times its ERH was reproducible within a few percent. Put together, these results indicate that efflorescence in ammonium nitrate droplets ~8 mm in diameter prepared from water solutions is determined by heterogeneous nucleation on impurity sites. The number of these impurity particles must be rather small in order to explain the wide interparticle distribution of ERH.

To test whether the impurity source was the water or the ammonium nitrate, we prepared particles from solutions of ammonium nitrate dissolved in purge and trap grade methanol. The methanol-based solutions were then filtered through 20 nm pore size filters. The methanol-based solution droplets were captured in the electrodynamic balance and the methanol solvent was evaporated off under vacuum, leaving a crystalline ammonium nitrate particle. After deliquescence in a water environment, it was found that over 90% of particles generated from the methanol solutions did not effloresce even when the water pressure was below 10^{-5} Torr. These anhydrous ammonium nitrate droplets were suspended for over 24 h at 0% RH without crystallizing; instead the highly volatile anhydrous droplets evaporate.

We conclude that the wide ranges of efflorescence points reported in the literature and observed in the present study are due to heterogeneous nucleation on unknown impurities that are present in every one of the water sources used. As pointed out by Vonnegut,[60] contamination by heterogeneous nuclei is less of a problem in smaller droplets as the probability of containing nuclei within a droplet decreases with particle volume. In two of the three literature studies that did not observe efflorescence,[41,59] the reported particle sizes were much smaller than the particles used in the present study. Thus it is likely that a large fraction of the particles observed in these studies did not contain an efficient nucleus. In the third study by Richardson and Hightower,[43] the authors note that only a small fraction of the ~6 mm diameter particles they produced remained liquid to low pressures, in agreement with our results for ammonium nitrate particles produced from water-based solutions. The two studies that did report efflorescence,[38,40] used particles generated from water solution that were at least as large as the particles used in the present study, and thus were highly likely to be influenced by heterogeneous nuclei. Our experiments with particles prepared from methanol solutions indicate that in the absence of impurities (with respect to heterogeneous efflorescence), efflorescence does not occur in ~8 mm diameter solution droplets of ammonium nitrate at 0% RH.

TABLE 2: Effects of Succinic Acid on Ammonium Nitrate

composn	no. of particles	%DRH	%ERH[a]	M/M_0	%RH for complete SA dissoln	no. of H_2O to dissolve SA[b]
NH_4NO_3	6	61.8 ± 0.3		1.54		
12.5% SA	7	61.4 ± 0.4	42.6 ± 1.8	1.45	~80	65
25% SA	7	61.0 ± 0.3	44.3 ± 0.7	1.41	~90	65
50% SA	7	60.6 ± 0.4	44.8 ± 0.8	1.21	~97[c]	

[a] Heterogeneous nucleation. [b] Calculated from the point where no efflorescence is observed. [c] Calculated from the no. of H_2O/SA from the two previous cases.

TABLE 3: Classical Nucleation Interpretation of Experimental Data

composn	impurity size (mm)	S^{*a}	I^b	$I_0{}^b$	W^*/kT	g^*	θ (deg)	n^*
NH_4NO_3		3.00	8.6×10^4	$\sim 1 \times 10^{32}$	62.8	114	180	
12.5% SA	3.1	1.79	3.24×10^6	2.66×10^{26}	45.8	157	65.3	97
25% SA	4.1	1.69	1.93×10^6	2.99×10^{26}	46.5	177	61.4	107
50% SA	5.2	1.65	1.18×10^6	3.18×10^{26}	47.1	189	59.6	113

[a] Critical supersaturation. [b] For the ammonium nitrate case I and I_0 will be J and J_0, respectively, and have the units of (cm^{-3} s^{-1}) instead of (cm^{-2} s^{-1}).

3.2.2. Ammonium Nitrate/Succinic Acid/Water. The sensitivity of the efflorescence transitions in ammonium nitrate/water droplets to impurities is clearly evident from the above discussion. It is therefore not surprising to find that the presence of succinic acid in ammonium nitrate droplets has a profound effect on efflorescence behavior. One must consider two very different efflorescence behavior regimes in a mixed ammonium nitrate/succinic acid/water particle depending on whether the succinic acid completely dissolves.

As long as the RH is kept below the critical value where all of the succinic acid is dissolved, a solid seed is present. Therefore, as the RH is decreased below the DRH a mixed AN/SA droplet becomes supersaturated with respect to ammonium nitrate, while the succinic acid seed grows by precipitation. Efflorescence occurs when the supersaturation reaches the critical value necessary to induce heterogeneous nucleation of ammonium nitrate on the succinic acid seed. Heterogeneous efflorescence points for each AN/SA composition are presented in Table 2. We note that the ERH is above 40% RH for all cases and that the interparticle variations are less than ±2% RH. The diameters of the solid succinic acid inclusions for each AN/SA composition, calculated assuming a spherical seed and by accounting for the small loss of succinic acid due to its solubility in water, are given in Table 3. This increase in surface area, and therefore in the number of potential nucleation sites, with the succinic acid composition going from 12.5% to 50% SA by mass increases the efflorescence rate and thus decreases the observed supersaturation necessary for efflorescence. The critical supersaturation, S^*, of the aqueous ammonium nitrate with respect to crystalline ammonium nitrate is obtained directly from the experimental data (see Figure 4), using the Gibbs−Duhem relation

$$\ln S^* = -\int_{\mathrm{DRH}}^{\mathrm{ERH}} x_1/x_2 \, \mathrm{d} \ln \mathrm{RH} \qquad (2)$$

where x_1/x_2 is the mole ratio of water to ammonium nitrate in the droplet.[32,61] This calculation is done assuming the small amount of dissolved succinic acid does not affect the ammonium nitrate supersaturation. The natural logarithm of the critical supersaturation is thus the area under the individual curves, when plotted in mole fraction vs lnRH, integrated from the natural logarithm of the deliquescence relative humidity to the efflorescence relative humidity. These supersaturations, presented in Table 3, illustrate the trend of decreasing S^* (increasing ERH) with increasing succinic acid composition.

A qualitatively different behavior is observed for runs in which the RH was raised above the critical RH where all of the succinic acid dissolves. A previous study on single suspended succinic acid solution droplets has reported an ERH of ~55%.[49] However, upon dehydration of a mixed AN/SA droplet, crystallization of either component is not observed to occur down to 0% RH. In this case there is a barrier to nucleation of both ammonium nitrate and succinic acid. This is illustrated in Figure 6 where the observed ERH for 25% by mass succinic acid mixed AN/SA particles are shown in a plot of ERH as a function of the maximum RH reached during a run. The observed efflorescence points (7−3) are consistently ~44% RH until the RH is raised to the point where the entire succinic acid seed is dissolved and no solids are present in the homogeneous solution droplet. With no seed to induce heterogeneous efflorescence, the particle remains in a liquid state to ~0% RH.

The composition of the particle near the maximum RH needed to fully dissolve the succinic acid can be estimated from results such as those shown in Figure 6 for particle compositions of 12.5% and 25% SA. For example, in Figure 6, the RH needed to fully dissolve the succinic acid is ~90% (point 1). The point labeled 2 in Figure 6 corresponds to a run that effloresced heterogeneously, either due to a contaminate present within the initial droplet or a small solid succinic acid core that did not fully dissolve. Due to this uncertainty we choose point 1 in Figure 6 as the critical point to fully dissolve all succinic acid. The ratio of water molecules to succinic acid at the critical RH is a measure of the solubility of the succinic acid within the solution. Our calculated solubilities for the 12.5% and 25% SA particle compositions given in Table 2 are in reasonable agreement with the reported solubility of succinic acid (SA) in the literature, 76 H_2O/SA.[20]

The Mie scattering spectra in Figure 7 provide supporting evidence for the above interpretation. Figure 7A illustrates the Mie spectrum of a 12.5% by mass succinic acid mixed AN/SA solution droplet during the evaporation phase of the cycle. At ≤60% RH a high-frequency signal indicating the presence of a succinic acid seed within the particle shows up on top of the regular Mie pattern. The heterogeneous nucleation event at ~41% RH confirms its presence. Figure 7B shows the Mie spectrum of an evaporating 25% by mass mixed AN/SA particle. What differentiates this run from the one shown in Figure 7A

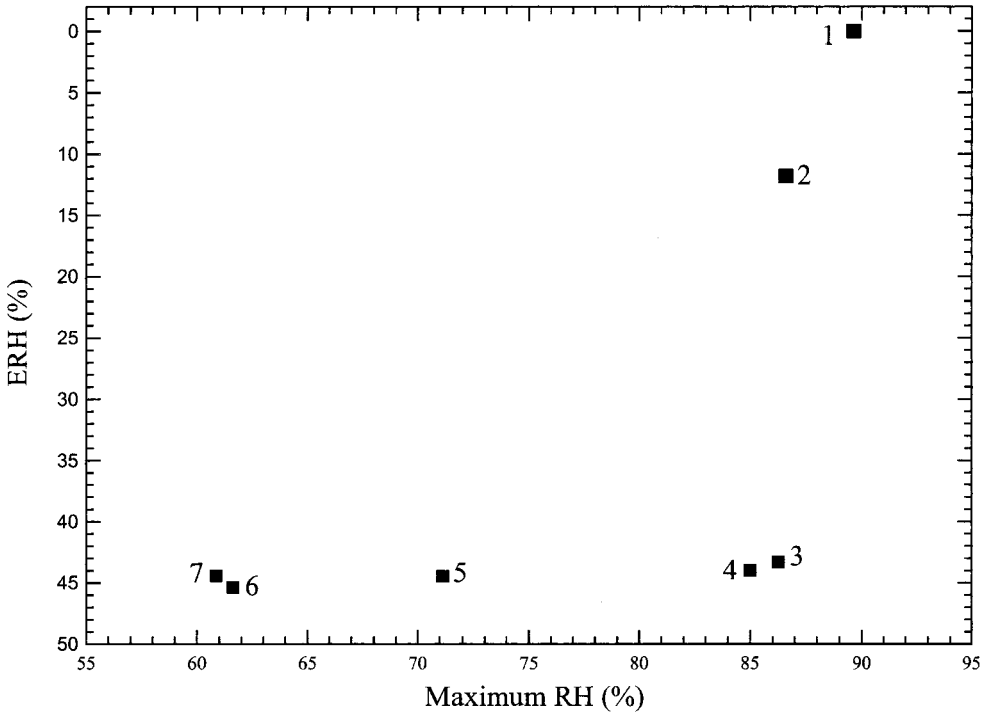

Figure 6. Relative humidity of efflorescence dependence on the maximum RH reached during an experiment. These points were obtained using mixed AN/SA particles with 25% SA by mass.

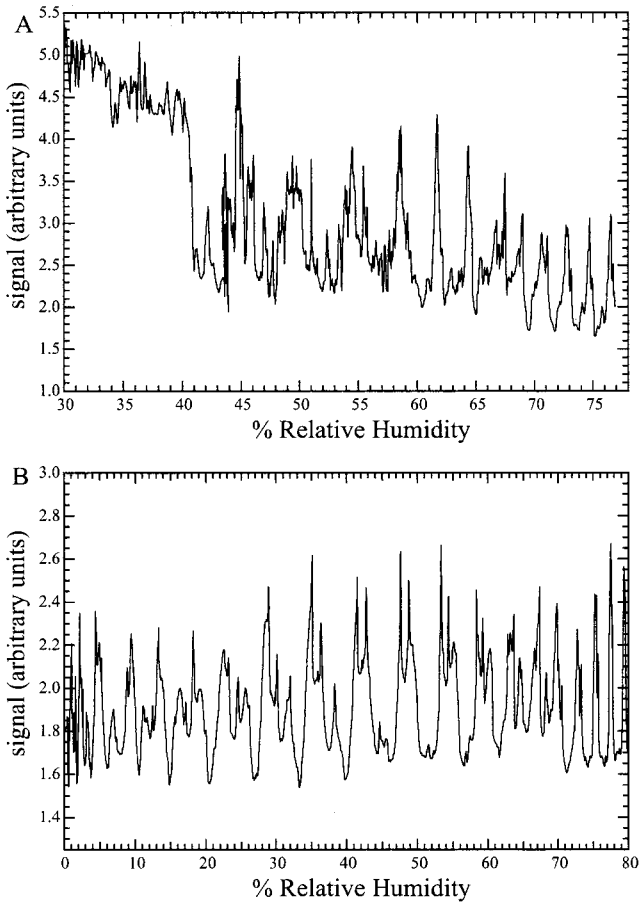

Figure 7. Mie-scattering versus decreasing RH for (A) an AN/SA (12.5%) particle with a solid SA inclusion, and (B) an AN/SA (25%) particle with the SA fraction dissolved. Note that the x-axes of (A) and (B) have different scales.

is the fact that maximum RH reached during this run was sufficiently high to completely dissolve the succinic acid seed. The homogeneous droplet produced a clear Mie spectrum devoid of the high-frequency component seen in Figure 7A, down to 0%RH. This specific particle never crystallized.

3.2.3. Analysis Using Nucleation Theory. The heterogeneous efflorescence of tertiary ammonium nitrate/succinic acid/water microparticles described above can be analyzed using classical nucleation theory. The general formulation[32,62,63] for the heterogeneous nucleation rate per unit area of the catalytic inclusion (cm^{-2} s^{-1}) is

$$I = I_0 \, e^{-W^*/kT} \tag{3}$$

where I_0 is a prefactor that represents the attempt frequency for a molecule of ammonium nitrate in solution to transition to the solid ammonium nitrate phase, W^* is the barrier height at the nucleation transition, k is Boltzmann's constant, and T is the temperature in kelvin. The heterogeneous nucleation rates, I, for each AN/SA case are estimated to be one event per unit surface area of the solid succinic acid inclusion per induction time of $t \leq 1$ s. The rates are calculated using $I = 1/(S_a t)$, where S_a is the surface area of the solid succinic acid inclusion given in Table 3 and the induction time is estimated from the rate of change of RH during an experiment.

In order to explicitly solve for I_0 and W^* in eq 3, we follow the derivation of the spherical cap model given by Richardson and Snyder.[61] This model assumes the critical nucleus to be a hemispherical cap that forms on the flat solid surface of the succinic acid inclusion and decreases the barrier height by a factor $f = (\cos \theta^3 - 3 \cos \theta + 2)/4$, where θ is the contact angle between the critical nucleus of solid ammonium nitrate and the organic substrate. The nucleation barrier height, W^*, is then described by

$$W^* = \frac{16\pi\sigma^3 v^2 f}{3(kT \ln S^*)^2} \tag{4}$$

where v is the molecular volume in the solid and σ is the surface

tension between the solid ammonium nitrate critical cluster and the solution.[61] In addition, I_0 can be written as

$$I_0 = n^*\left(\frac{\sigma}{kT}\right)^{1/2}\left(\frac{2v}{9\pi v_L^{\,2}}\right)^{1/3} f^{1/6}\nu \exp\left(\frac{-\Delta g}{kT}\right) \qquad (5)$$

where n^* is the number of molecules on the upper surface of the embryo, v_L is the molecular volume of the saturated ammonium nitrate solution,[38] ν is the jump frequency of the molecules in solution to the embryo (6.2×10^{12} Hz), and Δg is the free energy barrier of the jump. We use $\exp(-\Delta g/kT) \sim 2 \times 10^{-3}$ as estimated by Richardson and Snyder[61] for various salt solutions.

Combining eqs 3−5 gives an equation in terms of I, S^*, σ, and θ. I has been calculated above and S^* is determined from experimental data using eq 2 leaving an equation in terms of only the surface tension, σ, and the contact angle, θ. Assuming the surface tension, σ, between the solid ammonium nitrate critical cluster and the solution remains the same for both the ammonium nitrate and the mixed AN/SA, the surface tension can be estimated from the homogeneous efflorescence case of ammonium nitrate ($\theta = 180°$) in the following manner. For homogeneous nucleation, eq 3 becomes

$$J = J_0\, e^{-W^*/kT} \qquad (6)$$

where J is the volume-dependent homogeneous rate, J_0 ($\sim 10^{32}$ cm^{-3} s^{-1})[61] is the exponential prefactor, and W^* is the nucleation barrier height. The homogeneous rate is taken to be $J = (1/Vt)$, where V is the volume of the solution droplet and t is the longest observation time ($\sim$12 h). We estimate $J \sim 8.6 \times 10^4$ cm^{-3} s^{-1}. Since ammonium nitrate droplets did not homogeneously effloresce in this study, we can only determine an upper limit on the homogeneous efflorescence rate, J, and thus a lower limit on σ. The critical supersaturation, S^*, is calculated using eq 2 and the theoretical water uptake curve for ammonium nitrate.[3] The surface tension is then calculated from eqs 4 and 6 to be 38 ergs/cm^2. With this lower limit for σ, the contact angles, θ, for the mixed solution droplets can be determined for each AN/SA ratio. Additionally, the size of the critical nucleus can be determined from the barrier height and the critical supersaturation

$$\frac{W^*}{kT} = \frac{1}{2}g^* \ln S^* \qquad (7)$$

where g^* is the number of molecules in the critical embryo.[64] All values derived from eqs 2−7 are presented in Table 3.

The data derived from eqs 3−7 illustrate the effects a solid succinic acid inclusion has on the nucleation behavior of a supersaturated ammonium nitrate droplet. While these values are only an estimate, due to the barrier height calculated for the homogeneous case, the qualitative trends observed will be unaffected. To our knowledge, no other studies have been done using organic compounds as nuclei for heterogeneous efflorescence of electrolytic solution droplets. However, past studies on heterogeneous nucleation using inorganic salts as solid inclusions[32,61,62,65] have found surface tensions, σ, ranging from 36 to 88 ergs/cm^2 and contact angles, θ, between 69° and 92°. Results from this study lie very close to the lower end of these ranges with a surface tension of 38 ergs/cm^2 and angles ranging from 60° to 62° for the differing AN/SA compositions. In addition, we note that succinic acid effectively acts to lower the nucleation barrier despite being an insoluble organic with an orthorhombic crystal structure as compared with ammonium nitrate monoclinic crystal structure[66] (see Table 4). These findings are similar to those of Oatis et al.[32] in which calcium carbonate was found to nucleate ammonium sulfate efficiently despite having a differing crystalline structure.

TABLE 4: Crystalline Parameters for Ammonium Nitrate and Succinic Acid[66]

case	Z^a	$a_0{}^b$	$b_0{}^b$	$c_0{}^b$	space group
NH_4NO_3	2	5.75	5.45	4.96	$D_{2h}{}^{13}$
succinic acid	2	5.10	8.88	7.61	$C_{2h}{}^5$

[a] Number of molecules in a unit cell. [b] Size of unit cell in angstroms.

4. Conclusions

Thermodynamic and kinetic effects of succinic acid on ammonium nitrate microparticles have been investigated. In order to quantify these effects, characterization of ammonium nitrate/water particles was achieved. The technique we developed for compensating for the evaporation of $NH_{3(g)}$ and $HNO_{3(g)}$ made it possible to derive a complete hydration−dehydration curve for ammonium nitrate particles at 298 K. The model predictions of Clegg et al.[3] are in good agreement with our data. Using ultrapure methanol as a delivery solvent we have shown that $\sim$8 μm diameter ammonium nitrate particles do not exhibit homogeneous efflorescence, but form an anhydrous-liquid state. Such a concentrated electrolyte solution has only been observed in particle form. This highly supersaturated state is found to be very sensitive to foreign nuclei surfaces and to readily and reproducibly crystallize to the more stable anhydrous crystalline ammonium nitrate in their presence. We have successfully developed a technique to produce supermicron-sized ammonium nitrate particles that do not effloresce, allowing for future investigations of the molecular properties of such a unique state of matter.

The presence of succinic acid in an ammonium nitrate microparticle has significant effects on the particle's hygroscopicity, phase transitions, and optical properties. The particle growth factor, defined here in terms of mass, is found to decrease as a function of increasing succinic acid concentration. The observed decrease in particle growth factor is proportional to the increase in succinic acid concentration. Therefore, an atmospheric particle 25% succinic acid by mass will take up approximately 75% of the amount of water a pure ammonium nitrate particle of the same mass will absorb at deliquescence. This suggests that slightly soluble organic compounds, such as succinic acid, that have not completely dissolved do indeed exhibit the general behavior of insoluble solid components. Such results corroborate field measurements on ambient aerosol in which the observed water uptake, found to be lower than predicted by inorganic salt aerosol models, has been accredited to the presence of organic components. However, small effects on the thermodynamics of ammonium nitrate particles due to succinic acid's slight solubility are evident. For example, mixed AN/SA particles take up slightly more water than ammonium nitrate particles due to the presence of dissolved succinic acid and if the RH is taken high enough can fully dissolve the succinic acid forming a homogeneous liquid solution droplet. Furthermore, a slight trend of decreasing DRH with increasing succinic acid composition was observed.

The dominant effect of the succinic acid is on the efflorescence phase transitions of ammonium nitrate particles. The presence of a solid succinic acid particle successfully lowers the barrier to ammonium nitrate efflorescence. As the concentration of succinic acid increases, the ERH increases and the supersaturation decreases. In contrast, if the RH is high enough to dissolve the succinic acid within the particle, a homogeneous

solution droplet is formed and no efflorescence is observed down to 0% RH. This suggests that although the succinic acid is highly supersaturated, the presence of ammonium nitrate may inhibit nucleation of succinic acid crystals. These results indicate that the amount and solubility of slightly soluble components and the RH history of a particle are essential in order to successfully model mixed composition aerosol particles in the atmosphere. In particular, the dependence of the phase of a particle on small slightly soluble inclusions has important implications for the optical properties of atmospheric particles. Deliquescent particles grow with increasing RH and the increased volume greatly increases the amount of light scattered by these particles. If a deliquescent particle is contaminated by a solid organic inclusion, the particle may not remain hygroscopic at low RH due to a higher ERH and thus exist as a small crystalline particle. Thus, in the present case, however, the phase and hence volume and light scattering cross section of an ammonium nitrate particle intimately depend on whether succinic acid is internally mixed or not.

The heterogeneous efflorescence of AN/SA mixed particles was analyzed using classical nucleation theory. The resulting data are found to be similar in magnitude to previous studies involving inorganic species as the heterogeneous nuclei, despite the use of an organic in our case. We believe this to be the first heterogeneous nucleation study using solid organic compounds.

Acknowledgment. This work was supported by the U.S. Department of Energy (Contract DE-AC02-98CH10886). J.M.L. acknowledges an Energy Research Undergraduate Laboratory Fellowship sponsored by the U.S. Department of Energy Office of Science, and the Science Education Department of Brookhaven National Laboratory. T.B.O. acknowledges an Alexander Hollaender Distinguished Postdoctoral Fellowship sponsored by the U.S. Department of Energy, Office of Biological and Environmental Research, and administered by the Oak Ridge Institute for Science and Education. S.O. acknowledges the support of the National Science Foundation Atmospheric Chemistry Program (Grant no. ATM-9806111).

References and Notes

(1) Lammel, G.; Pohlmann, G. *J. Aerosol Sci.* **1992**, *23*, S941−S944.
(2) Gordon, R. J.; Bryan, R. J. *Environ. Sci. Technol.* **1973**, *7*, 645−647.
(3) Clegg, S. L.; Brimblecombe, P.; Wexler, A. S. *J. Phys. Chem.* **1998**, *102*, 2137−2154.
(4) Gray, H. A.; Cass, G. R.; Huntzicker, J. J.; Heyerdahl, E. K.; Rau, J. A. *Environ. Sci. Technol.* **1986**, *20*, 580−589.
(5) Novakov, T.; Penner, J. E. *Nature* **1993**, *365*, 823.
(6) Sloane, C. S.; Watson, J.; Chow, J.; Pritchett, L.; Richards, L. W. *Atmos. Environ.* **1991**, *25A*, 1013.
(7) Forstner, H. J. L.; Flagan, R. C.; Seinfeld, J. H. *Atmos. Environ.* **1997**, *31*, 1953.
(8) Forstner, H. J. L.; Flagan, R. C.; Seinfeld, J. H. *Environ. Sci. Technol.* **1997**, *31*, 1345−1358.
(9) Pandis, S. N.; Harley, R. A.; Cass, G. R.; Seinfeld, J. H. *Atmos. Environ.* **1992**, *26A*, 2269−2282.
(10) Blando, J. D.; Porcja, R. J.; Li, T.-H.; Bowman, D.; Lioy, P. J.; Turpin, B. J. *Environ. Sci. Technol.* **1998**, *32*, 604−613.
(11) Schroder, B.; Stoffregen, J.; Dannecker, W. *J. Aerosol Sci.* **1991**, *22*, S669−S672.
(12) Cautreels, W.; Van Cauwenberghe, K. *Atmos. Environ.* **1976**, *10*, 447−457.
(13) Rogge, W. F.; Hildemann, L. M.; Mazurek, M. A.; Cass, G. R. *Environ. Sci. Technol.* **1998**, *32*, 13−22.
(14) Grosjean, D. *Environ. Sci. Technol.* **1989**, *23*, 1506−1514.
(15) Kawamura, K.; Kaplan, I. R. *Environ. Sci. Technol.* **1987**, *21*, 105−112.
(16) Kawamura, K.; Ikushima, K. *Environ. Sci. Technol.* **1993**, *27*, 2227−2235.
(17) Grosjean, D.; Van Cauwenberghe, K.; Schmid, J. P.; Kelley, P. E.; Pitts, J. J. N. *Environ. Sci. Technol.* **1978**, *12*, 313−317.
(18) Sempere, R.; Kawamura, K. *Atmos. Environ.* **1994**, *28*, 449.
(19) Sempere, R.; Kawamura, K. *Atmos. Environ.* **1996**, *30*, 1609.
(20) Saxena, P.; Hildemann, L. *J. Atmos. Chem.* **1996**, *24*, 57−109.
(21) Ansari, A. S.; Pandis, S. N. *Environ. Sci. Technol.* **2000**, *34*, 71−77.
(22) Saxena, P.; Hildemann, L. M.; McMurry, P. M.; Seinfeld, J. H. *J. Geophys. Res.* **1995**, *100*, 18755−18770.
(23) Hameri, K.; Rood, M.; Hansson, H.-C. *J. Aerosol Sci.* **1992**, *23*, S437−S440.
(24) Hansson, H.-C.; Wiedensohler, A.; Rood, M. J.; Covert, D. S. *J. Aerosol Sci.* **1990**, *21*, S241−S244.
(25) Xiong, J. Q.; Zhong, M.; Fang, C.; Chen, L. C.; Lippmann, M. *Environ. Sci. Technol.* **1998**, *32*, 3536−3541.
(26) Chen, Y.-Y.; Lee, W.-M. G. *Chemosphere* **1999**, *38*, 2431−2448.
(27) Hameri, K.; Charlson, R. J.; Hansson, H.-C.; Jacobson, M. *J. Aerosol Sci.* **1998**, *29*, S587−S588.
(28) Hameri, K.; Charlson, R. J.; Hansson, H.-C.; Jacobson, M. *J. Aerosol Sci.* **1997**, *28*, S153.
(29) Andrews, E.; Larson, S. M. *Environ. Sci. Technol.* **1993**, *27*, 857−865.
(30) Brooks, S. D.; Prenni, A. J.; Wise, M. E.; Tolbert, M. A. *AGU Fall Meeting Abstr.* **1999**, *A21A-02*.
(31) Han, J.; Martin, S. T. *J. Geophys. Res.* **1999**, *104*, 3543−3553.
(32) Oatis, S.; McGraw, R.; Imre, D.; Xu, J. *Geophys. Res. Lett.* **1998**, *25*, 4469−4472.
(33) Tang, I. N.; Munkelwitz, H. R. *Atmos. Environ.* **1993**, *27A*, 467−483.
(34) Tang, I. N.; Munkelwitz, H. R. *J. Geophys. Res.* **1994**, *99*, 18801−18808.
(35) Tang, I. N.; Fung, K. H. *J. Chem. Phys.* **1997**, *106*, 1653−1660.
(36) Wexler, A. S.; Seinfeld, J. H. *Atmos. Environ.* **1990**, *24A*, 12331−12346.
(37) Mamane, Y.; Pueschel, R. F. *Atmos. Environ.* **1980**, *14*, 629−639.
(38) Tang, I. N. *J. Geophys. Res.* **1996**, *101*, 19,245−19,250.
(39) Tang, I. N. Deliquescence Properties and Particle Size Change of Hygroscopic Aerosols. In *Generation of Aerosols and Facilities for Exposure Experiments*; Willeke, K., Ed.; Ann Arbor Science Pub. Inc.: Ann Arbor, MI, 1980; pp 153−165.
(40) Chan, C. K.; Flagan, R. C.; Seinfeld, J. H. *Atmos. Environ.* **1992**, *26A*, 1661−1673.
(41) Cziczo, D. J.; Abbatt, J. P. D. *J. Phys. Chem.* **2000**, *104A*, 2038.
(42) Edgar, G.; Swan, W. O. *J. Am. Chem. Soc.* **1922**, *44*, 570−577.
(43) Richardson, C. B.; Hightower, R. L. *Atmos. Environ.* **1987**, *21*, 971−975.
(44) Harrison, R. M.; Sturges, W. T.; Kitto, A.-M. N.; Li, Y. *Atmos. Environ.* **1990**, *24A*, 1883−1888.
(45) Larson, T. V.; Taylor, G. S. *Atmos. Environ.* **1983**, *17*, 2489−2495.
(46) Stelson, A. W.; Seinfeld, J. H. *Atmos. Environ.* **1982**, *16*, 993−1000.
(47) Stelson, A. W.; Seinfeld, J. H. *Atmos. Environ.* **1982**, *16*, 2507−2514.
(48) Harris, D. C. *Quantitative Chemical Analysis*, 3rd ed.; W. H. Freeman: New York, 1995.
(49) Na, H.; Arnold, S.; Myerson, A. S. *J. Cryst. Growth* **1995**, *149*, 229−235.
(50) McMurry, P. H.; Zhang, X.; Lee, C. *J. Geophys. Res.* **1996**, *101*, 19189−19197.
(51) Pitchford, M. L.; McMurry, P. H. *Atmos. Environ.* **1994**, *28*, 827−839.
(52) Tang, I. N.; Munkelwitz, H. R. *J. Appl. Meteorol.* **1994**, *33*, 791−796.
(53) Wexler, A. S.; Seinfeld, J. H. *Atmos. Environ.* **1991**, *25A*, 2731−2748.
(54) Tang, I. N.; Munkelwitz, H. R.; Davis, J. G. *J. Aerosol Sci.* **1978**, *9*, 505−511.
(55) Orr, J., Clyde; Hurd, F. H.; Corbett, W. J. *J. Colloid Sci.* **1958**, *13*, 472−482.
(56) Yaws, C. L.; Nijhawan, S. *Oil Gas J.* **1994**, *92*, 80.
(57) Stokes, R. H.; Robinson, R. A. *J. Phys. Chem.* **1966**, *70*, 2126−2131.
(58) Zhang, Y.; Seigneur, C.; Seinfeld, J. H.; Jacobson, M.; Clegg, S. L.; Binkowski, F. S. *Atmos. Environ.* **2000**, *34*, 117−137.
(59) Dougle, P. G.; Pepijn Veerkind, J.; Ten Brink, H. M. *J. Aerosol Sci.* **1998**, *29*, 375−386.
(60) Vonnegut. *J. Colloid Interface Sci.* **1948**, *3*, 563.
(61) Richardson, C. B.; Snyder, T. D. *Langmuir* **1994**, *10*, 2462−2465.
(62) Onasch, T.; Imre, D. Submitted for publication in *J. Phys. Chem.*
(63) Turnbull, D. J. *J. Chem. Phys.* **1952**, *20*, 411−424.
(64) McGraw, R.; Laaksonen, A. *Phys. Rev. Lett.* **1996**, *76*, 2754.
(65) Tang, I. N.; Munkelwitz, H. R. *J. Colloid Interface Sci.* **1984**, *98*, 430−438.
(66) Wyckoff, R. W. G. *Crystal Structures*, 1st ed.; Interscience: New York, 1960; Vol. IV.